



E-ISSN: 2278-4136

P-ISSN: 2349-8234

www.phytojournal.com

JPP 2020; 9(4): 1660-1665

Received: 19-05-2020

Accepted: 21-06-2020

Ketsemen H Landry

Department of Organic Chemistry, Faculty of Science, the University of Yaounde 1, BP 812 Yaounde-Cameroon

Awantu A Fusi

Department of Chemistry, Faculty of Science, The University of Bamenda, Cameroon

Omdim N Irène

Department of Organic Chemistry, Faculty of Science, the University of Yaounde 1, BP 812 Yaounde-Cameroon

Shafi U Khan

Department of Pharmacy, COMSATS University of Information Technology, Abbottabad, Pakistan

Qazi N Us Saqib

Department of Pharmacy, COMSATS University of Information Technology, Abbottabad, Pakistan

Folefoc N Gabriel

Department of Organic Chemistry, Faculty of Science, the University of Yaounde 1, BP 812 Yaounde-Cameroon

Eyong O Kenneth

Department of Organic Chemistry, Faculty of Science, the University of Yaounde 1, BP 812 Yaounde-Cameroon

Reverse-docking study of a new indeno[1,2-b]pyran skeleton: Target investigation

Ketsemen H Landry, Awantu A Fusi, Omdim N Irène, Shafi U Khan, Qazi N Us Saqib, Folefoc N Gabriel and Eyong O Kenneth

Abstract

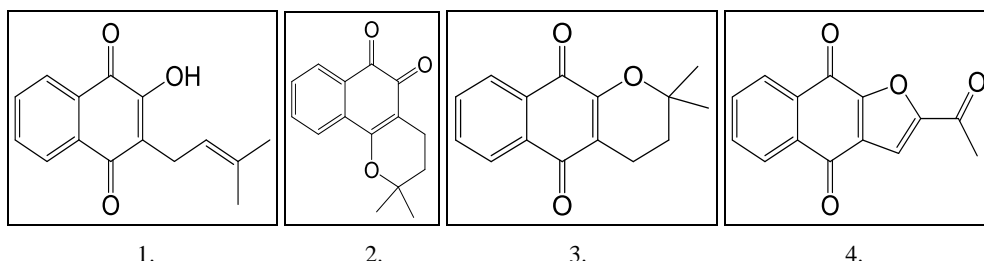
The reverse-docking of a new indeno[1,2-b] pyran skeleton on a panel of 25 protein targets is described. Reverse-docking analysis was performed by using AutoDockTools-1.5.6. The parameters used for the docking analysis are binding energy (ΔG), inhibition constant (K_i), Van der waals energy (vdw), torsional energy (Tors), intermolar energy (U) and H-Bond interactions (binding affinity). The 25 targets were retrieved from Protein Data Bank in pdb format. The comparative inhibition activity was analyzed by inhibition constant (K_i) and H-Bond interactions. The reverse-docking analysis reveals that the Vascular Endothelial Growth Factor Receptor 2 protein (VEGFR2) followed by the Disintegrin and Metalloprotease protein (ADAMTS-5) gave the best binding affinities and could therefore be the biological targets of this new indeno[1,2-b] pyran skeleton. Three other proteins, the Cyclin-dependent kinase 9 (CDK9), the Serine/threonine-protein kinase (PLK-2) and the Receptor tyrosine-protein kinase (HER2) showed that they could also be involved with small contributions in the whole antiproliferative activity of compound 5.

Keywords: Indeno-pyran, reverse-docking, anti-proliferative, binding affinity, autodock4

Introduction

Cancer is the uncontrolled growth of abnormal cells in the body. Cancer develops when the body's normal control mechanism stops working. Old cells do not die and instead grow out of control, forming new, abnormal cells. These extra cells may form a mass of tissue, called a tumor. One in five men and one in six women worldwide will develop cancer during their lifetime, and almost one in six deaths worldwide is due to cancer^[1]. Although effective on the tumor response, chemotherapy treatments are not without consequences. Indeed, they can present toxicities which can lead to deterioration in the quality of life.

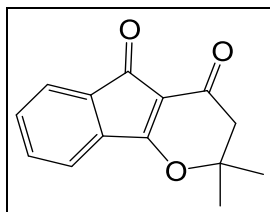
In the search for new bioactive molecules with anticancer activity, we carried out phytochemical studies on *Kigelia Africana*, *Markhamia stipulata*, *Stereospermum kunthianum*, *Stereospermum acuminatissimum*, *Newbouldia laevis*^[2]. Plants of the Bignoniaceae family. This study resulted in the isolation of many compounds amongst which lapachol (1) has been the most active^[3]. The first detailed anticancer effects of lapachol were evaluated in 1968^[4] and this compound was shown to possess very potent effects toward cancerous tumors in rats^[3]. Historically, chemical transformation of the lapachol scaffold has yielded new derivatives with impressive biological activity and rich chemical diversity. β -lapachone (2), α -lapachone (3) and 2-acetylfuronaphthoquinone (4) are examples of analogs derived from lapachol that show superior antitumor activity compared to the natural product.

**Corresponding Author:****Ketsemen H Landry**

Department of Organic Chemistry, Faculty of Science, the University of Yaounde 1, BP 812 Yaounde-Cameroon

In a pharmacomodulation attempt to remove the quinone groups, which is generally associated with undesirable effects, including acute cytotoxicity, immunotoxicity, and carcinogenesis^[5, 6], orthoquinones were converted to indene-pyran derivatives via benzylic acid rearrangement. To avoid these potential pitfalls associated with drugs that possess a quinone moiety. We unexpectedly obtained a 1, 3 indene-pyran di-one (5). This compound showed potent

cytotoxic activity and eliminated virtually all cells in culture (close to 0% cell viability) at concentrations just slightly exceeding its IC₅₀ value [7].



5

Considering the good activity associated with this compound (5) and the fact that this scaffold has not been the object of any cancer study, we sought to find out by virtual screening possible biological targets and therefore the mode of action mechanism.

Virtual screening-based drug designs have successfully resulted in some approved drugs in recent history and the technique used to this end is molecular docking which is a one-target (protein or enzyme) many ligand (small molecule) concept [8]. A docking program predicts the binding mode of a small molecule/target protein complex. In order to find the most plausible binding modes, the docking program ranks possible conformations using a scoring function. Reverse docking is a method that does the opposite of direct docking.

That is a one-ligand many-target protein complex [8]. With the list of ranked target proteins, the relevance of a given ligand for particular diseases or its side effects can be estimated. Therefore, the reverse docking method is useful in finding activities of new drugs or for drug repositioning. This procedure looks for natural products of which the exact effects are not yet known such as compound (5) and also for new targets of drugs already approved.

Materials and Methods

Reverse Molecular docking studies

Preparation of Ligand

The 3D molecular structure of compound (5) was generated using Chem3D 15.0 running a windows workstation with an Intel(R) Core (TM) i5-3340M processor. The 3D structures of the compound was then saved in .pdb format. It was imported to the workspace and preparation was done for docking studies. The docking results of different targets were compared against the corresponding crystalized complex and listed in descending order.

Preparation of Enzyme

To perform reverse docking of compound (5), a panel of twenty five targets was selected based on their function in the cellular life. These targets are summarize in the table 1 below and the 3D structures were obtained from protein data bank (<http://www.rcsb.org>) in .pdb format.

Table 1: Some enzyme targets in Cancer therapy

Function	Targets
Targets involved in cell proliferation	HER2, IGF-1R, HSP90, ADAMTS-5, C-Src, PI3K, AKT, mTOR
Targets involved in tumor vascularization	ITK, VEGFR-2
Targets involved in the cell cycle	CDK5, CDK6, CDK7, CDK9, CHK1, CHK2, Aurora A, Aurora C, PLK2
Targets involved in repairing DNA damage	PARP
Targets involved in the apoptosis mechanism	BCL-2
Histone deacetylase inhibitors	HDAC1, HDAC2, HDAC3

The AutoDockTools [9] (ADT) was used to prepare the ligand and receptor structures, add appropriate Gasteiger and Kollman charges, identify and modify ligand rotatable bonds [10]. The potential binding sites of target were calculated using the Lamarckian GA (4.2) algorithm implemented in Autodock4 [11]. The population size, maximum number of evaluation (medium) and maximum number of generations were set at 150, 27 000 and 2 500 000 respectively [12]. The search space of the simulation exploited in the docking studies was studied as a subset region of the active site containing the co-crystallized ligand. The water molecules were removed from the enzyme to decrease interactions between functional group of ligands and water molecules. AutoDock program performs the research and evaluation of the different ligand configurations. It is possible to use several techniques to obtain the configurations (by simulated annealing, genetic algorithm or by Lamarckian genetic algorithm). A grid-based method was used to enhance the quick evaluation of the binding energy of conformations of

the complexes formed. The grid boxes were centered using coordinates of a virtual center of mass atom for the enzymes [14]. For each protein, the grid box was determined respectively in x, y and z dimension according to amino acids which formed active site. The affinity of the docked complexes was described using inhibition constant (K_i) and binding energy based on a semi empirical force field [9].

Results

The ability of compound (5) to bind with a particular target is given in terms of binding energy. The binding energy and inhibition constants are used as the parameters for analyzing the docking results. The protein targets are ranked according to their binding energy. The proteins possessing the lowest binding energy show a strong affinity for the target.

The important results of *in-silico* reverse-docking analysis of compound (5) on the twenty five selected proteins ranking based on binding energy and inhibition constant are presented in Table 2.

Table 2: Summarises the docking results of each selected protein with its natural ligand and the reverse docking of compound 5 with these proteins.

Target	Protein code	Natural ligand code (L0)	Ligand name	Estimated $\Delta G_{\text{Binding}}$ (L0) (kcal/mol)	Inhibition constant Ki (L0) (μM)	Estimated $\Delta G_{\text{Binding}}$ (kcal/mol)	Inhibition constant Ki (μM)
VEGFR2	3vhe	42Q	1-{2-FLUORO-4-[(5-METHYL-5H-PYRROLO[3,2-D]PYRIMIDIN-4-YL)OXY]PHENYL}-3-[3-(TRIFLUOROMETHYL)PHENYL]UREA	-11.59	0.00322	-7.86	1.72
ADAMTS-5	2rjq	BAT	4-(N-HYDROXYAMINO)-2R-ISOBUTYL-2S-(2-THIENYLTHIOMETHYL)SUCCINYL-L-PHENYLALANINE-N-METHYLAMIDE	-7.61	2.63	-7.79	1.95
PI3K	1e7v	LY2	2-MORPHOLIN-4-YL-7-PHENYL-4H-CHROMEN-4-ONE	-8.55	0.64814	-7.67	2.4
Top 1	1t8i	EHD	4-ETHYL-4-HYDROXY-1,12-DIHYDRO-4H-2-OXA-6,12A-DIAZA-DIBENZO[B,H]FLUORENE-3,13-DIONE/CAMPTOTHECIN	-10.37	0.02487	-7.54	2.95
mTOR	4jsp	AGS	PHOSPHOTHIOPHOSPHORIC ACID-ADENYLATE ESTER	-7.5	3.18	-7.36	4
PARP	4l6s	1WQ	(2S)-6-[[4-(4-CHLOROPHENYL)-3,6-DIHYDROPYRIDIN-1(2H)-YL]METHYL]-2-METHYL-2H-1,4-BENZOXAZIN-3(4H)-ONE	-9.95	0.0505	-7.34	4.19
AKT	2uzt	SS3	(2S)-1-[[5-(3-METHYL-1H-INDAZOL-5-YL)PYRIDIN-3-YL]OXY]-3-PHENYLPROPAN-2-AMINE	-10.93	0.00981	-7.25	4.84
BCL2	2o2f	LIO	4-(4-BENZYL-4-OXYMETHYLEPIPERIDIN-1-YL)-N-[[4-[[1,1-DIMETHYL-2-(PHENYLTHIO)ETHYL]AMINO]-3-NITROPHENYL]SULFONYL]BENZAMIDE	-10.72	0.01379	-7.17	5.56
IGF-1R	3o23	MQY	(5S)-5-METHYL-1-(QUINOLIN-4-YLMETHYL)-3-{4-[(TRIFLUOROMETHYL)SULFONYL]PHENYL}IMIDAZOLIDINE-2,4-DIONE	-11.13	0.00693	-7.09	6.31
CDK5	3o0g	3O0	{4-AMINO-2-[(4-CHLOROPHENYL)AMINO]-1,3-THIAZOL-5-YL}(3-NITROPHENYL)METHANONE	-10.37	0.02504	-7.07	6.61
ITK	4l7s	G7K	TRANS-4-({4-[DIFLUORO(4-FLUOROPHENYL)METHYL]-6-[(5-METHOXY[1,3]THIAZOLO[5,4-B]PYRIDIN-2-YL)AMINO]PYRIMIDIN-2-YL}AMINO)CYCLOHEXANOL	-9.57	0.09585	-7.07	6.63
CDK9	3tn8	F18	4-[(E)-(3,5-DIAMINO-1H-PYRAZOL-4-YL)DIAZENYL]PHENOL	-5.64	73.4	-7.04	6.93
HSP90	2xhr	COP	4-CHLORO-6-[2,4-DICHLORO-5-(2-MORPHOLIN-4-YLETHOXY)PHENYL]PYRIMIDIN-2-AMINE	-8.93	0.28278	-7.01	7.32
Aurora C	6gr9	VX6	CYCLOPROPANECARBOXYLIC ACID [4-[4-(4-METHYL-PIPERAZIN-1-YL)-6-(5-METHYL-2H-PYRAZOL-3-YLAMINO)-PYRIMIDIN-2-YLSULFANYL]-PHENYL]-AMIDE	-9.36	0.13687	-6.97	7.8
CDK6	4ez5	ORS	{5-[4-(DIMETHYLAMINO)PIPERIDIN-1-YL]-1H-IMIDAZO[4,5-B]PYRIDIN-2-YL}[2-(ISOQUINOLIN-4-YL)PYRIDIN-4-YL]METHANONE	-10.18	0.03448	-6.92	8.5
CHK1	1nvs	UCM	REL-(9R,12S)-9,10,11,12-TETRAHYDRO-9,12-EPOXY-1H-DIINDOLO[1,2,3-FG:3',2',1'-KL]PYRROLO[3,4-I][1,6]BENZODIAZOCINE-1,3(2H)-DION	-9.35	0.14101	-6.9	8.79
CDK7	1ua2	ATP	ADENOSINE-5'-TRIPHOSPHATE	-6.58	14.94	-6.8	10.42
PLK-2	4i6b	11G	(7R)-8-CYCLOPENTYL-7-ETHYL-5-METHYL-7,8-DIHYDROPTERIDIN-6(5H)-ONE	-6.62	14.01	-6.76	11.02
CHK2	2xk9	XX9	N-{4-[(1E)-N-(N-HYDROXYCARBAMIMIDOYL)ETHANEHYDRAZONOYL]PHENYL}-7-NITRO-1H-INDOLE-2-CARBOXAMIDE	-9.57	0.09631	-6.75	11.19
C-Src	4u5j	RXT	(3R)-3-CYCLOPENTYL-3-[4-(7H-PYRROLO[2,3-D]PYRIMIDIN-4-YL)-1H-PYRAZOL-1-YL]PROPANENITRILE	-6.72	11.89	-6.72	11.96
Aurora A	3h10	97B	9-CHLORO-7-(2,6-DIFLUOROPHENYL)-N-{4-[(4-METHYLPIPERAZIN-1-YL)CARBONYL]PHENYL}-5H-PYRIMIDO[5,4-D][2]BENZAZEPIN-2-AMINE	-9.76	0.06978	-6.59	14.89
HDAC3	4a69	IOP	D-MYO INOSITOL 1,4,5,6 TETRAKISPHOSPHATE	-15.45	0.00000475	-6.58	15.01

HDAC2	3max	LLX	N-(4-AMINOBIHENYL-3-YL)BENZAMIDE	-10.58	0.01745	-6.56	15.45
HDAC1	5icn	I6P	INOSITOL 1,2,3,4,5,6-HEXAKISPHOSPHATE	-14.44	0.00002613	-6.17	29.87
HER2	1n8z	NAG	N-ACETYL-D-GLUCOSAMINE	-5.4	109.42	-5.72	64.08
ADAMTS-5	2rjq	NAG	N-ACETYL-D-GLUCOSAMINE	-4.98	223.44	-5.37	116.72

Discussion

Table 2 shows 25 proteins with binding energy between $\Delta = -5.37$ kcal/mole and $\Delta = -7.86$ kcal/mol. The Vascular Endothelial Growth Factor Receptor 2 protein (VEGFR2) showed lower binding energy $\Delta = -7.86$ kcal/mole than the other proteins followed by the Disintegrin and Metalloprotease protein ADAMTS-5 ($\Delta = -7.86$ kcal/mole) in one of its two active sites. But the binding energy of the VEGFR2-compound 5 complex is higher than that of VEGFR2-co-crystallized complex ($\Delta = -11.59$ kcal/mole) when the binding energy of the ADAMTS-5-compound 5 complex is less (BAT: $\Delta = -7.79$ kcal/mole, NAG: $\Delta = -5.37$ kcal/mole) than that of the ADAMTS-5-co-crystallized complex (BAT: $\Delta = -7.61$ kcal/mole, NAG: $\Delta = -4.98$ kcal/mole) showing that these two targets should be both considered for experimental validation.

The affinity of the VEGFR2-compound 5 complex (Figure 1) is manifested by one hydrogen bond interaction of the carbonyl of the pyrane moiety with the amino acid residue

LYS A:868, Alkyl and Pi-Alkyl interactions with the amino acid residues ALA A:866, VAL A:916, LEU A:889 and VAL A:914, one Carbon Hydrogen bond interaction with PHE A:1047 and one Pi-Sigma interaction with LEU A:1035.

The affinity of the ADAMTS-5-compound 5 complex (BAT Pocket) (Figure 2) is manifested by three hydrogen bond interactions: two between the carbonyl of the indene moiety and the amino acid residues Leu A:379 and GLY A:380 and one between the oxygen of the ether of the pyran moiety and LEU A:443, one Pi-Cation interaction with HIS A:410, Alkyl and Pi-Alkyl interactions with the amino acid residues LEU A:379, LEU A:443 and ILE A:442, two Carbon Hydrogen bond interactions with THR A:378 and ILE A:442.

The affinity of the ADAMTS-5-compound 5 complex (NAG Pocket) (Figure 3) is manifested by two hydrogen bond interactions of both the two carbonyls with the amino acid residue TYR A:491, one Pi-Sigma interaction with GLY A:286 and Alkyl and Pi-Alkyl interactions with the amino acid residues LEU A:499 and TYR A:283.

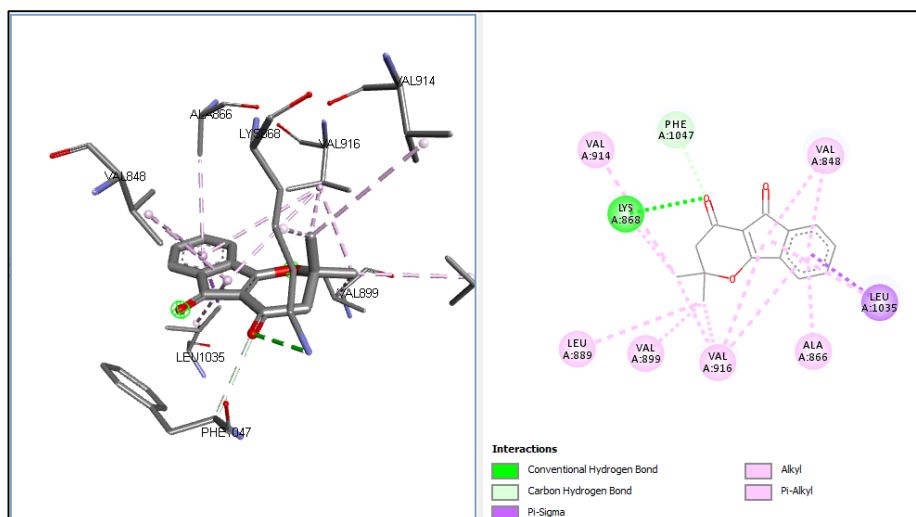


Fig 1: 3-dimensional and 2-dimensional results of docking of compound 5 in VEGFR protein

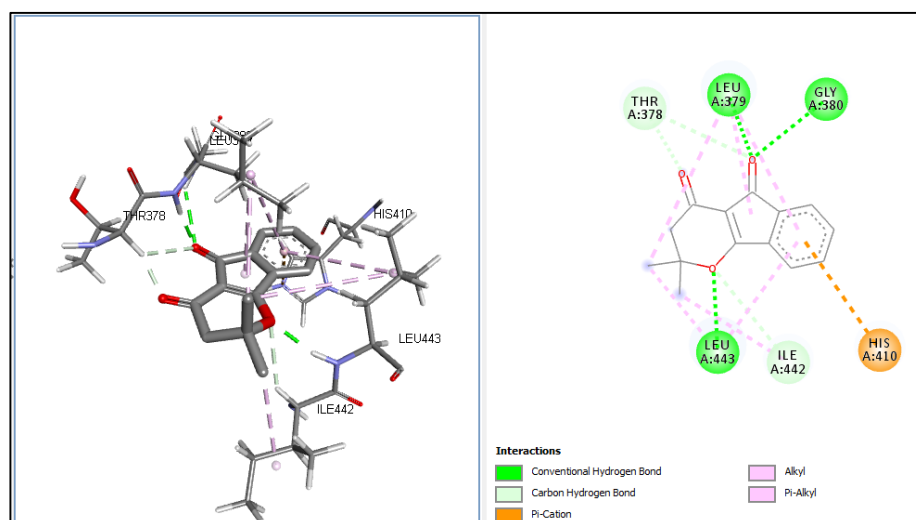


Fig 2: 3-dimensional and 2-dimensional results of docking of compound 5 in ADAMTS-5 protein (BAT Pocket)

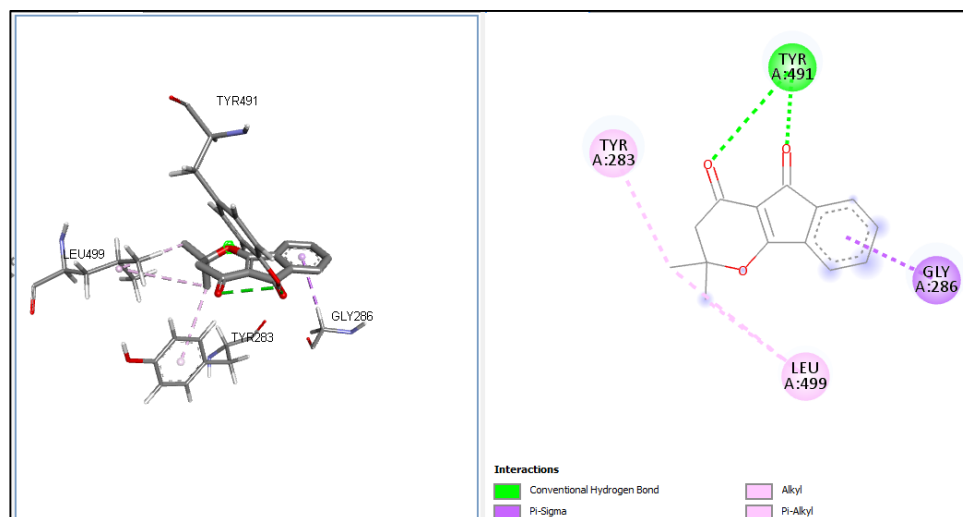


Fig 3: 3-dimensional and 2-dimensional results of docking of compound 5 in ADAMTS-5 protein (NAG Pocket)

Beside these two best values of binding affinities, there are three others protein-compound 5 complex with relatively high binding energy, but less compared to the corresponding protein-co-crystalized ligand. There are Cyclin-dependent kinase 9 (CDK9) (CDK9-compound 5: $\Delta = -7.04$ kcal/mole, CDK9-F18: $\Delta = -5.64$ kcal/mole), Serine/threonine-protein kinase (PLK-2) (PLK-2-compound 5: $\Delta = -6.76$ kcal/mole, PLK-2-11G: $\Delta = -6.62$ kcal/mole) and Receptor tyrosine-protein kinase (HER2) (HER2-compound 5: $\Delta = -5.72$ kcal/mole, HER2-NAG: $\Delta = -5.4$ kcal/mole). These three proteins can therefore be possible targets of small side effects which add small contributions to the whole antiproliferative activity of compound 5.

Conclusion

In summary, reverse-docking analysis of a new indeno[1,2-b]pyran skeleton was performed on 25 protein targets. The docking score and binding patterns were compared with that of the co-crystalized ligand of each protein. The proteins VEGFR2 and ADAMTS-5 were the most active and thus could therefore be consider for *in-vitro* enzymatic validation as the biological targets of compound (5). The affinities of compound (5) with the proteins HER2, CDK9 and PLK-2 are also comparable to the affinities of these proteins with their co-crystallization ligands. These proteins can therefore also be involved in the activity of compound (5). Further studies can be performed to validate our docking results through *in-vitro* screening , to discover pharmacokinetic properties, to know the absorption, distribution, metabolism and excretion of this new antiproliferative indeno[1,2-b]pyran skeleton.

Acknowledgements

The authors thank the Faculty of Science of the University of Yaounde I, the Third World Academy of Sciences (TWAS) for sponsoring the fellowship Mr Ketsemen at the COMSATS University of Abbotabad in Pakistan and the Government of Cameroon for financial support through the 'Fonds d'Appuis a la Recherche'.

References

1. WHO. Cancer <https://www.who.int/fr/news-room/factsheets/detail/cancer> (accessed Jun 3, 2020).
2. Eyong KO, Ketsemen HL, Ghansenyuy SY, Folefoc GN. Chemical Constituents, the Stereochemistry of 3-Hydroxy Furonaphthoquinones from the Root Bark of *Newbouldia laevis* Seem (Bignoniaceae), and Screening

against *Onchocerca ochengi* Parasites. *Med. Chem. Res.* 2015, 24(3):965-969. <https://doi.org/10.1007/s00044-014-1173-z>.

3. Hussain H, Krohn K, Ahmad V, Miana G, Green I. Lapachol: An Overview. *Arkivoc*, 2007.
4. Nepomuceno JC. Lapachol and Its Derivatives as Potential Drugs for Cancer Treatment. In *Plants and Crop The Biology and Biotechnology Research*; iConcept Press Ltd, 2014, 19.
5. Bolton JL, Trush MA, Penning TM, Dryhurst G, Monks TJ. Role of Quinones in Toxicology. *Chem. Res. Toxicol.* 2000; 13(3):135-160.
6. Monks TJ, Hanzlik RP, Cohen GM, Ross D, Graham DG. Quinone Chemistry and Toxicity. *Toxicol. Appl. Pharmacol.* 1992; 112(1):2-16. [https://doi.org/10.1016/0041-008X\(92\)90273-U](https://doi.org/10.1016/0041-008X(92)90273-U).
7. Eyong KO, Ketsemen HL, Zhao Z, Du L, Ingels A, Mathieu V *et al.* Antiproliferative Activity of Naphthoquinones and Indane Carboxylic Acids from Lapachol against a Panel of Human Cancer Cell Lines. *Med. Chem. Res.* 2020; 29:1058-1066. <https://doi.org/10.1007/s00044-020-02545-0>.
8. Kharkar PS, Warriar S, Gaud RS. Reverse Docking: A Powerful Tool for Drug Repositioning and Drug Rescue. *Future Medicinal Chemistry. Future Science* 2014, 333-342. <https://doi.org/10.4155/fmc.13.207>.
9. Morris GM, Ruth H, Lindstrom W, Sanner MF, Belew RK, Goodsell DS *et al.* Software News and Updates AutoDock4 and AutoDockTools4: Automated Docking with Selective Receptor Flexibility. *J Comput. Chem.* 2009; 30(16):2785-2791. <https://doi.org/10.1002/jcc.21256>.
10. Model M SJ, MG. undefined. Python: A Programming Language for Software Integration and Development. *academia.edu*. 1999,
11. Autodock A, Morris G, Goodsell D, Halliday R. Automated Docking Using a Lamarckian Genetic Algorithm and an Empirical Binding Free Energy Function, 1998.
12. Bahadori MB, Dinparast L, Valizadeh H, Farimani MM, Ebrahimi SN. Bioactive Constituents from Roots of *Salvia syriaca* L.: Acetylcholinesterase Inhibitory Activity and Molecular Docking Studies. *South African J. Both.* 2016; 106:1-4. <https://doi.org/10.1016/j.sajb.2015.12.003>.

13. Robien MA, Bosch J, Buckner FS, Van Voorhis WCE, Worthey EA, Myler P Mehlin *et al.* Crystal Structure of Glyceraldehyde-3-Phosphate Dehydrogenase from *Plasmodium Falciparum* at 2.25 Å Resolution Reveals Intriguing Extra Electron Density in the Active Site. *Proteins Struct. Funct. Bioinforma.* 2005; 62(3):570-577. <https://doi.org/10.1002/prot.20801>.
14. Forlemu N, Watkins P, Sloop J. Molecular Docking of Selective Binding Affinity of Sulfonamide Derivatives as Potential Antimalarial Agents Targeting the Glycolytic Enzymes: GAPDH, Aldolase and TPI. *Open J Biophys.* 2017; 07(01):41-57. <https://doi.org/10.4236/ojbiphy.2017.71004>.